

Drawing parameters influence on the hardness of a steel bar analysed by simulation

Darlan Vale Bayão¹ 
Ana Luísa Camargos Barcelos¹ 
Geraldo Magno Mól Ferreira¹ 
Túlio César Nogueira¹ 
Mariana Machado da Silveira¹ 
Ermani Vinicius de Oliveira Lima² 
João Pedro Moreira Silva³ 
Alisson Duarte da Silva^{3*} 
Ricardo Antônio Micheletti Viana³ 

Abstract

This study investigates the influence of drawing parameters on the final hardness profile of thermally untreated drawn bars. By analyzing the mechanical behavior of the material through experimental tests and computational simulations using QForm UK software, the research explores the relationships between plastic strain, hardness variation, and process parameters. Results indicate that parameters such as die semi-angle and wire rod diameter significantly affect hardness distribution and mechanical properties. A predictive methodology for correlating plastic strain with hardness is proposed, offering valuable insights for optimizing the drawing process and improving manufacturing efficiency.

Keywords: Bar drawing; Hardness; Simulation; Finite elements.

1 Introduction

A mechanical component needs to achieve the necessary specifications to perform well in its application. The mechanical strength of the material is one of the main control requirements. Therefore, hardness tends to be the main mechanical property of reference in specific regions of the final part.

The drawing process is one of the oldest mechanical forming methods, in which the raw material is forced through a die that shapes it and provides a good surface finish [1]. In this way, like all cold forming processes, the material that is deformed changes its mechanical properties because of the hardening that happens during the process. Observing Hollomon's equation, it can be seen that stress values are high for small deformations [2]. This effect is called strain hardening. In general, softer steels are desirable in wire drawing, as they reduce the loads placed on the equipment and increase the life of the dies [3].

However, softer, low-carbon materials can make it difficult to achieve higher hardnesses, either by heat treatment or strain hardening. Thus, a good selection of raw material is necessary. For example, for drawing followed by quenching

it may be desirable to add alloying elements, or for a process without heat treatment it may be desirable to have a higher mechanical strength in the workpiece material. In fact, in a drawing process with strict control, the quality of the raw material has a direct influence on the final component. In the occasion that there is no heat treatment, this quality becomes even more important.

The finite element method has become widely accepted as a tool of choice for simulating forming processes and assessing the effect of process parameters [4]. This approach is adopted in this study, where the characteristics of a drawn bar are correlated with its hardness properties. Mechanical tests were conducted on both the wire rod and the drawn bar, and the drawing processes were simulated using QForm UK software (Micas Simulation Ltd., Oxford, UK). These simulations utilized test data to determine the material's behavior and to compare practical results with simulated outcomes. The study investigated how key parameters in the drawing process influence the billet's hardness profile, ultimately proposing methodologies to predict the final hardness.

¹ArcelorMittal Sabará, Sabará, MG, Brasil.

²ArcelorMittal Monlevade, João Monlevade, MG, Brasil.

³Sixpro, Belo Horizonte, MG, Brasil.

*Corresponding author: alisson@sixpro.pro

Adresses: darlanvalebayao@gmail.com; ana.barcelos@arcelormittal.com.br; geraldomagnomol.ferreira@arcelormittal.com.br; tulio.nogueira@arcelormittal.com.br; ermani.vo.lima@arcelormittal.com.br; mariana.m.silveira@arcelormittal.com.br; joaopedro201148@gmail.com; ricardo@sixpro.pr



2 Methodology

Mechanical tests were conducted on both the wire rod and the drawn bar, and the drawing processes were simulated using QForm UK software (Micas Simulation Ltd., Oxford, UK). The test data were used to determine the material's behavior and to compare the practical hardness results with the simulated plastic strain profiles. The investigation considered various wire rod diameters and different die semi-angles to understand how these parameters influence the billet's hardness profile. Flow stress curves were obtained through compression tests, and the results were integrated into the simulations. To estimate the final hardness based on plastic deformation, the study proposes fitting a curve that describes the relationship between plastic strain and hardness, creating a methodology for predicting the material's final mechanical properties.

2.1 Hardness testing procedure

The hardness tests were performed using a diamond pyramid indenter with a square base. The applied force was 1,961 N, and no attack was applied during testing. The tests were conducted at a temperature of 20.8 °C, with an increase of 400x magnification for better observation. A 200 g load was used, and the tests followed the ABNT NBR NM ISO 6507-1:2019 [5] standard. The hardness was measured from the edge to the core of the sample using an Optical Microhardness Tester Wolpert Model 62279. The distance from the first indentation to the edge was 0.18 mm, and the distance between subsequent indentations was 1.15 mm.

2.2 Bar drawing

Drawn bars made of SAE 10B30 steel, also named PL30D in wire drawing manufacturing, with their typical chemical composition shown in Table 1, are cut to specific lengths to

be used as billets for cold forging, among other possibilities. Therefore, the drawing process of this material was considered, which starts from a 20.64 mm diameter hot-rolled wire rod and is formed in just one pass to a 19.05 mm in diameter drawn bar.

Using a spinneret with a 15° semi-angle, α , the simulation of the drawing process is presented in Figure 1. The image includes photographs of some of the compression-tested specimens, indicating the region of withdrawal of these samples, before and after drawing. From the compression tests, the flow stress curves (in MPa) of the wire rod and the drawn bar were obtained as a function of the plastic strain, defined by Equations 1 and 2. The simulation was based on the wire rod's flow stress curve, disregarding the effects of strain velocity and temperature, and used a hybrid friction condition, with a 0.05 friction coefficient and a 0.10 friction factor.

$$\sigma_{FM} = 401 + 550 \cdot \phi^{0.22} \tag{1}$$

$$\sigma_{BT} = 512 + 470 \cdot \phi^{0.26} \tag{2}$$

Since wire drawing is a cold-forming process, the wire rod undergoes strain hardening [6]. However, the hardness profile is not uniform in the drawn bar, as it can be seen from the plastic strain profile shown in Figure 2. The plastic strain ranged from 0.19 to 0.37 along the diameter of the drawn bar, as shown in Figure 3.

Despite the minimal plastic strain found in the bar, the uniform plastic strain, ϵ_u , necessary to obtain the reduction founded is 0.16 according with the equation (Equation 3). In addition to the ideal work, there is work against friction between workpiece and tools, and work to do redundant or unwanted deformation [7], it was observed that the strain used in the drawing was greater, which can be defined as a

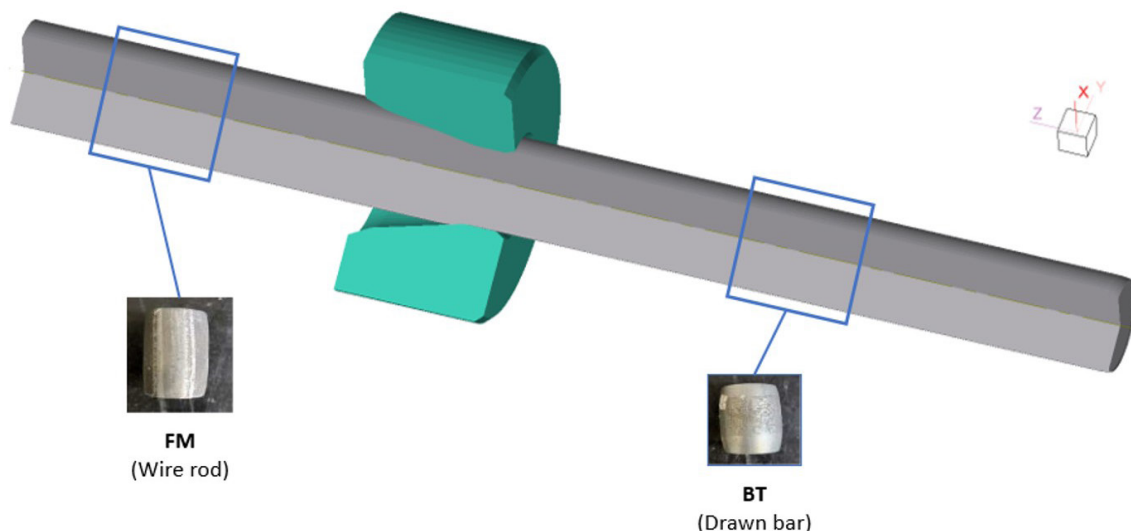


Figure 1. Simulation of the drawing of a bar, indicating the region of sampling for experimental compression tests.

Table 1. Chemical Composition (%p) of SAE 10B30 Steel

Component	S	C	Mn	P	Si	Al	Cr	B	N	Ti	Fe
Min.	0.000	0.300	0.800	0.000	0.150	0.020	0.300	0.001	0.000	0.020	Bal.
Max	0.007	0.340	1.000	0.020	0.300	0.080	0.400	0.003	0.006	0.040	Bal.

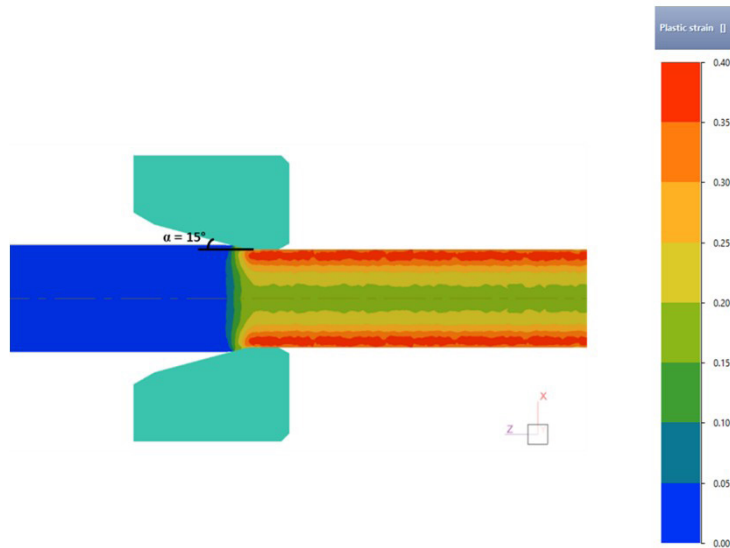


Figure 2. Prediction of plastic strain in the drawn bar (longitudinal section).

redundant strain and can be observed based on the distortion of the line matrix after passing through the die (Figure 4). Redundant strain occurs due to the geometry of the die, which distorts the material and therefore increases the strain, which is necessary for an economically viable process. If the deformation were ideal, plane sections would with straight lines. In real processes, the surface layers are sheared relative to the center. The material undergoes more strain than required for the diameter reduction and consequently strain hardens more and is less ductile [7].

$$\phi_u = \ln \left(\frac{A_0}{A_f} \right) \quad (3)$$

The wire rod yield curve (Equation 1) is plotted in the Figure 5, under which it is possible to quantify the work required to carry out the average drawing strain. In this graph, the areas for the calculation of uniform work and redundant work were indicated and distinguished, and redundant work was limited to the final average plastic strain of 0.26 (Equation 4).

$$\bar{\epsilon}_{Tref} = \frac{\sum_{i=1}^n \epsilon_i}{n} \quad (4)$$

Considering the average plastic strain obtained in the drawn bar, it was plotted in the graph of Figure 6 the flow stress curve of the wire rod (Equation 1) and the flow curve

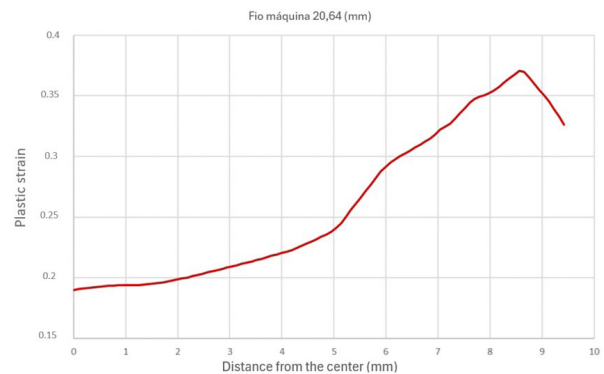


Figure 3. Prediction of plastic strain variation along the drawn bar radius.

of the drawn bar (Equation 2) shifted to start with 0.26 of strain. It was observed in practice that the initial yield stress of the drawn bar was not equivalent to the yield stress in the wire rod at that strain.

For comparison, a compression test was simulated on the drawn bar, using the same flow stress curve from the wire rod to the material, and this simulated test resulted in a flow stress curve in which the initial yield stress was equivalent to the stress on the wire rod flow stress curve.

In addition to the flow stress curves, hardness measurements were made along the radius for the wire rod and for the drawn bar (Figure 7), thus understanding the

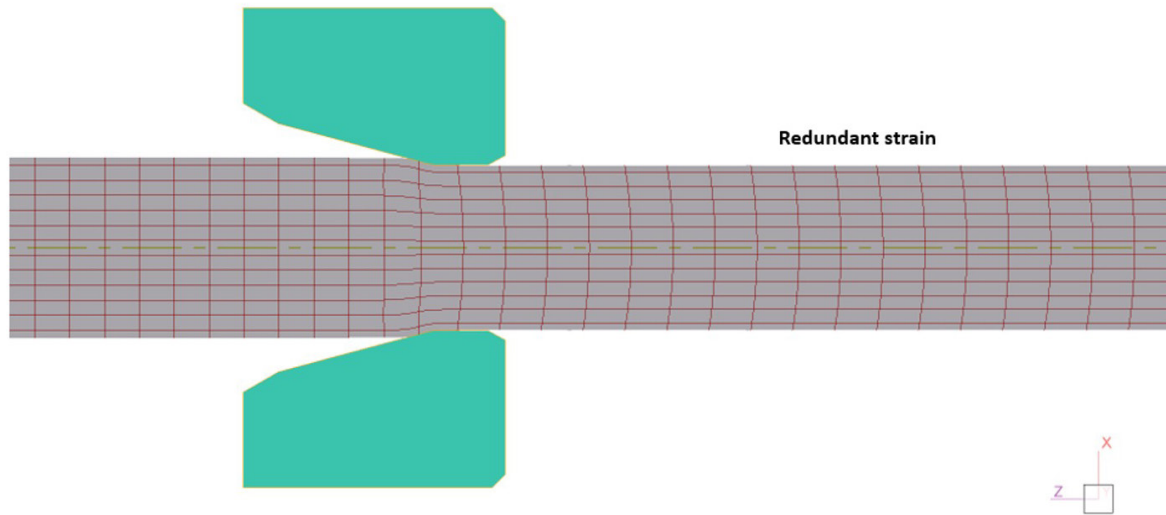


Figure 4. Redundant strain evidenced by distortion of the line matrix.

behavior of hardness (Figure 8). The Wire Rod showed a variation possibly due to the cooling rate after hot rolling, since the surface regions cool faster and, thus, reach relatively higher hardness. On the other hand, the drawn bar presented significantly higher hardness, due to the strain hardening, and maintained a trend of greater hardness in the regions closer to the surface, although the hardness variation was reduced in relation to the wire rod. The average hardness (Equation 5) was calculated for both cases, resulting in 204 HV for the wire rod and 243 HV for the drawn bar.

$$\bar{H} = \frac{\sum_{i=1}^n H_i}{n} \quad (5)$$

2.3 Changes in drawing

To exemplify the influence of drawing conditions on the mechanical strength of the bar, the variation of the following parameters was analyzed: die semi-angle and wire rod diameter. It is important to mention that several other aspects can influence the quality of the drawn bar, such as the lubrication condition, the drawing speed, the length of the parallel, the evolution of the wear of the spinneret, among others.

By varying the die semi-angle between 3 and 15°, it was observed that smaller semi-angles provide a more homogeneous plastic strain profile, as reported in Figure 9. Therefore, the average hardness in the bar section tends to decrease with the semi-angle decreasing.

In addition to the plastic strain profile, it was also observed the influence of the semi-angle on the drawing force, presented in Figure 10.

The resulting drawing force can be demonstrated as a composition of the force required to deform the bar uniformly, calculated on the basis of uniform strain (Figure 5), the force required to perform the redundant strain, obtained

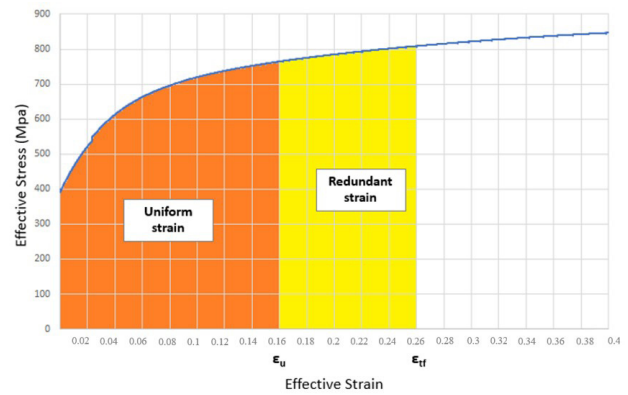


Figure 5. Work per unit volume carried out in the drawing process.

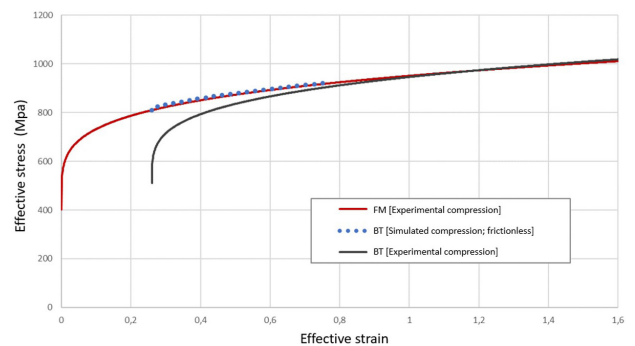


Figure 6. Wire rod (FM) and drawn bar (BT) flow stress curves.

from simulations with zero friction, and the force required to overcome the friction, obtained from the resulting difference. Thus, a range between 5 and 9° was found for lower drawing forces and, therefore, subject to energy savings.

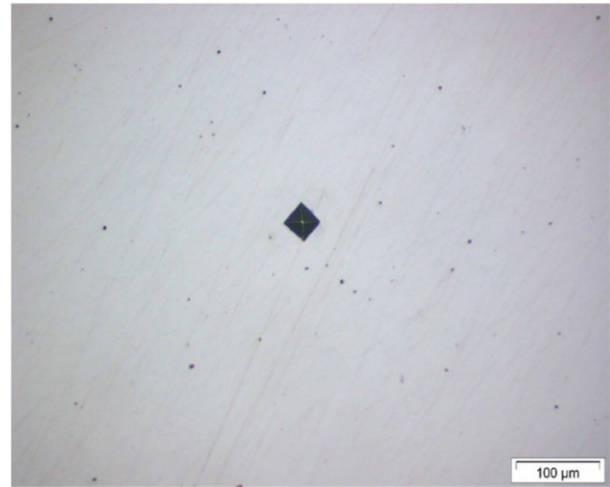
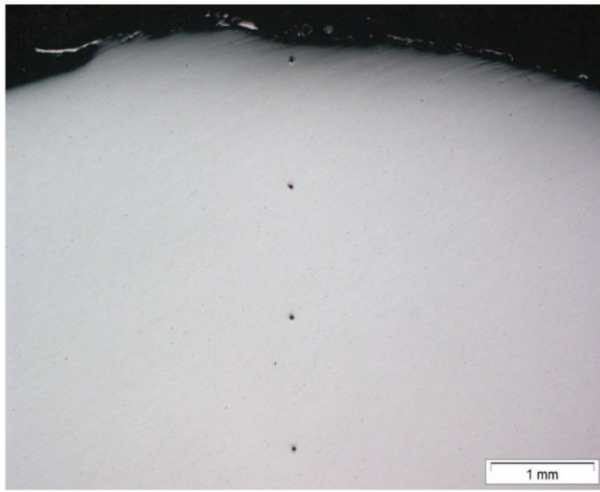


Figure 7. Hardness tests performed along the radius for the wire rod (FM).

The diameter of the wire rod is another parameter that can be adjusted and that significantly influences the strain of the drawn bar. By determining a die semi-angle of 7° and varying the diameter of the wire rod between 20.00 and 20.64 mm, the result is presented in the behavior of the plastic strain in the drawn bar in Figure 11. For comparison, considering the current process with a 15° semi-angle and a 20.64 mm diameter of the wire rod, the estimated decreasing of the average strain in the drawn bar for a process with a 7° semi-angle and a 20.00 mm diameter of the wire rod would be 0.06.

3 Results

3.1 Hardness prediction

The least squares method is widely recognized as one of the best techniques for curve fitting, providing an optimal solution by minimizing the sum of squared residuals between the observed and predicted values [8]. To correlate the plastic strain that occurred during the drawing process with the final hardness observed in the part, hardness measurements were performed at different points at different distances from the center of the drawn bar. These values were then associated with the plastic strain calculated using QForm UK software. In addition, the hardness value of the material before the drawing process was included. Using these data, the least squares method was used to fit a curve that best represented the points of interest, finding Equation 6. The results of these analyses are presented in Table 2 and Figure 12.

$$H = 660.6 \cdot \phi^3 - 737.3 \cdot \phi^2 + 299.3 \cdot \phi + 203.9 \quad (6)$$

Based on Equation 6, it was possible to make predictions about the variation of the hardness in function

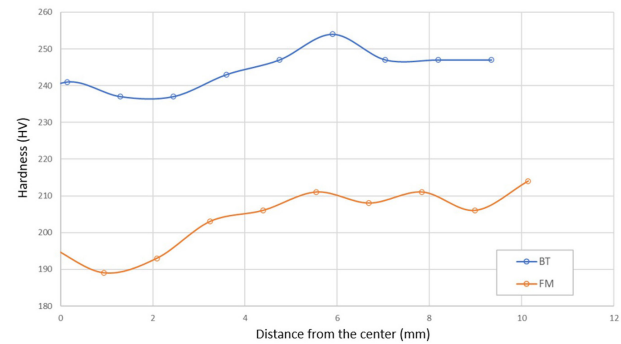


Figure 8. Hardness variation along the wire rod (FM) and drawn bar (BT) radiuses.

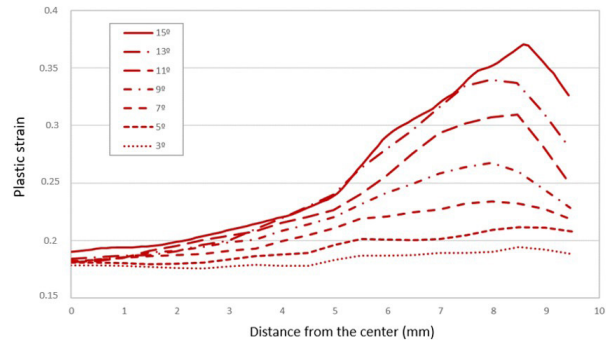


Figure 9. Prediction of plastic strain in the drawn bar for different die semi-angles.

of its plastic strain. The hardness profile was examined for die semi-angles between 3° and 15°, and wire rod diameter ranging from 20.00 mm to 20.64 mm. The upward trend in the hardness of the material is evident as both the die angle and wire rod diameter increase. This phenomenon is the result of the greater hardening imposed to the part with the

Table 2. Hardness prediction deviation

Position (mm)	Hardness (HV) (Experiment)	Plastic strain (Simulation)	Hardness (HV) (Simulation)	Hardness deviation
-	204	0.00	204	0.0%
0.1	241	0.19	239	0.8%
1.4	237	0.20	240	1.3%
2.4	237	0.20	240	1.3%
3.6	243	0.22	241	0.8%
4.7	247	0.24	242	2.0%
5.9	254	0.28	244	3.9%
7.0	247	0.32	246	0.4%
8.3	247	0.34	246	0.4%
9.3	247	0.27	244	1.2%

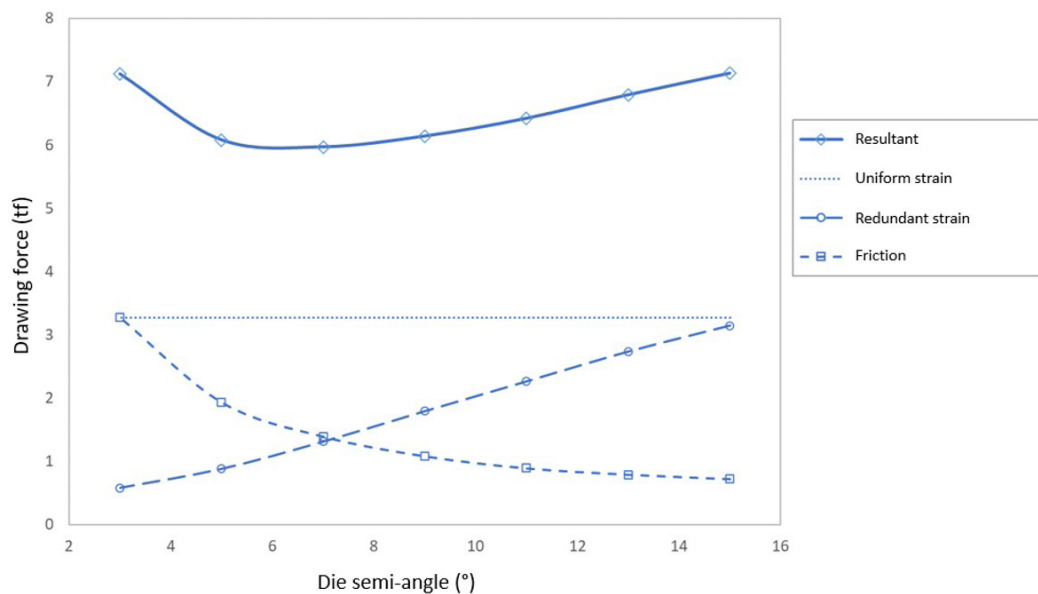


Figure 10. Resulting drawing force and its components as a function of die semi-angle.

increasing in the material volume, along with the speed at which this material deforms, influenced by the semi-angle. Figures 13, 14, 15 and 16 illustrate this relationship, showing that the estimated hardness ranged from approximately 229 HV to 247 HV, reflecting this observed trend.

4 Discussion

The semi-angle of the die was a critical factor in determining the final hardness of the proposed material, while the initial diameter of the wire had an insignificant impact. It is possible that the minimal variation of only 0.64 mm in diameter was responsible for this insignificant hardness variation, but this specific case was the focus of interest at the time of the study. The precise control of the semi-angle allowed for a more accurate prediction of the material’s performance characteristics, highlighting its importance in the manufacturing process to achieve desired mechanical

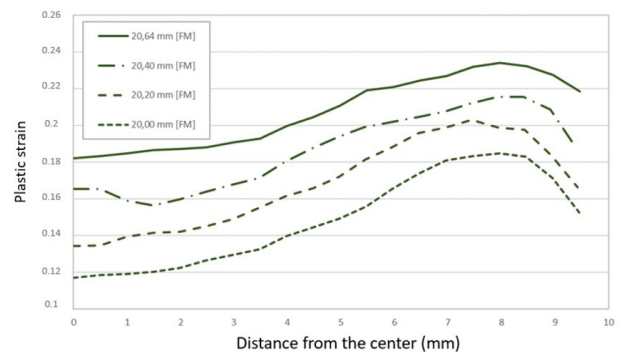


Figure 11. Prediction of plastic strain in the drawn bar for a 7° semi-angle and different diameters of the wire rod (FM).

properties. Furthermore, this correlation suggests that cost control can be achieved based on this study, as optimizing the semi-angle can lead to reduced energy consumption.

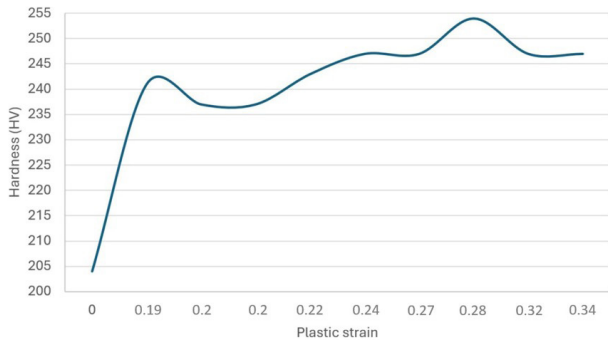


Figure 12. Correlation between measured hardness and simulated plastic deformation

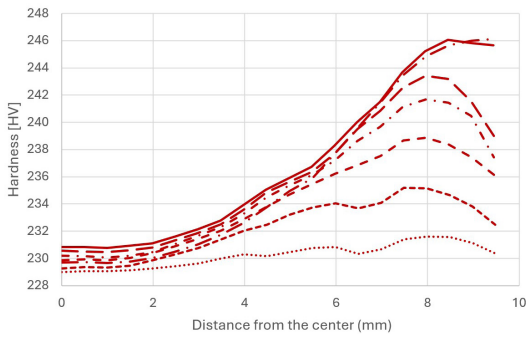


Figure 13. Hardness prediction for different semi-angles in a 20.00 mm diameter wire rod.

Further studies would be necessary to explore this aspect of diameter variation in greater detail. Adopting the best parameters derived from our results can contribute to more efficient manufacturing practices.

Additionally, we observed non-uniform deformation along the wire. This phenomenon raises questions about its relevance to the material's application, indicating that further studies are needed to understand the implications of this deformation on performance and durability in real-world scenarios.

While the results obtained from this study cannot be directly applied to other materials, the methodology employed can be analogously utilized. This flexibility in approach allows for broader applications in future research, encouraging the exploration of various materials under similar conditions to evaluate their properties and performance.

Moreover, the percentage variation between the simulated hardness and the maximum experimental hardness was found to be 3.9%. This variation can be attributed to the methodology and the proposed equations used as a predictive tool for hardness in this study. Such a deviation is considered acceptable within the intended engineering application field, reinforcing the reliability of the proposed approach in practical scenarios. The relatively low deviation further supports the applicability of the developed model in predicting material hardness with sufficient accuracy for industrial applications.

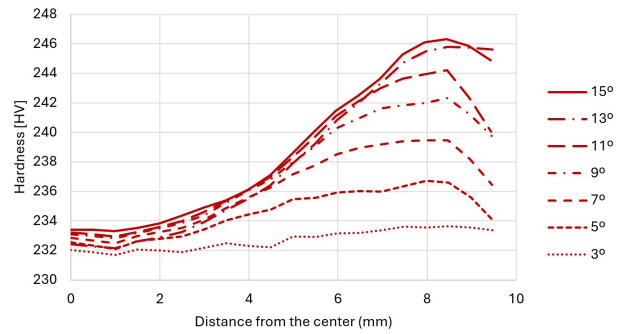


Figure 14. Hardness prediction for different semi-angles in a 20.20 mm diameter wire rod.

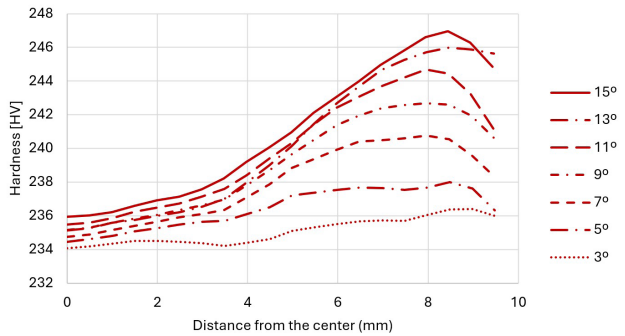


Figure 15. Hardness prediction for different semi-angles in a 20.40 mm diameter wire rod.

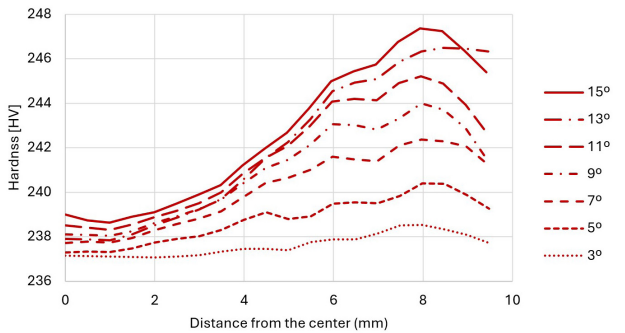


Figure 16. Hardness prediction for different semi-angles in a 20.64 mm diameter wire rod.

5 Conclusion

The conducted analyses emphasize the pivotal role of optimizing drawing parameters to achieve both compliance with required mechanical specifications and enhanced process efficiency.

The investigation revealed that the die semi-angle significantly impacts the hardness distribution and mechanical properties of the drawn bar, corroborating the findings by Zohdi [4], which highlighted the influence of forming geometry on material behavior during metal forming processes. Conversely, the minimal effect of wire

rod diameter on hardness variation aligns with observations by Hosford and Caddell [7].

The established correlation between plastic strain and hardness provides a robust predictive tool for understanding the effects of process modifications. Hardness prediction presented less than 4% deviation from the experiments, in special. Beyond process optimization, this correlation enables the development of more effective quality control strategies, ensuring consistency and reliability in the manufacturing of drawn bars, as highlighted by methodologies suggested by Press et al. [8].

Additionally, the study highlights non-uniform deformation along the wire, a phenomenon previously

discussed by Bresciani et al. [6], who associated similar effects with redundant strain caused by die geometry. This aspect invites further exploration to assess its implications on material performance and durability in practical applications.

Ultimately, this research contributes not only to advancing the understanding of mechanical forming processes but also to developing industry practices that prioritize precision, efficiency, and quality. The methodologies and insights presented can be extended to other materials and conditions, fostering broader applications and encouraging future research in material forming processes while providing practical tools.

References

- 1 Soares CAT. Análise das tensões residuais no processo de trefilação considerando os efeitos de anisotropia [dissertação]. Porto Alegre: Curso de Pós-graduação em Engenharia de Minas, Metalúrgica e de Materiais, UFRGS; 2010.
- 2 Cipriano GL. Determinação do coeficiente de encruamento de metais através da morfologia das impressões de dureza na escala macroscópica. Tese de Mestrado, Universidade Tecnológica Federal do Paraná, Curitiba; 2008.
- 3 Bayão DV, et al. Influência da trefilação na dureza de peças forjadas – uma análise integrada do processo. In: Anais do Seminário Nacional de Forjamento (SENAFOR) 2023; Porto Alegre; p. 199-210; 2023.
- 4 Zohdi TI. Finite element simulation of metal forming processes. Berlin: Springer; 2003.
- 5 Associação Brasileira de Normas Técnicas. ABNT NBR NM ISO 6507-1:2019 Materiais metálicos - Ensaio de Dureza Vickers. Rio de Janeiro: ABNT; 2019.
- 6 Bresciani E. Fo et al. Conformação plástica dos metais. 6. ed. São Paulo: UPUSP; 2011.
- 7 Hosford WF, Caddell RM. Metal forming: mechanics and metallurgy. Cambridge: Cambridge University Press; 2011.
- 8 Press WH, Teukolsky SA, Vetterling WT, Flannery BP. Numerical recipes: the art of scientific computing. 3rd ed. Cambridge: Cambridge University Press; 2007.

Received: 18 Oct. 2024

Accepted: 21 Feb. 2025

Editor-in-charge:

André Luiz Vasconcellos da Costa e Silva - 